Design and Optimization of Surface Plasmonic Sensor with Tunable Optical Actuation Angle based on Microsystems Technology for Microfluidic Application

Reza Mokhtarpour
Sahand University of Technology
Habib Badri Ghavifekr (badri@sut.ac.ir)
Sahand University of Technology https://orcid.org/0000-0003-2834-9821

Research Article

Keywords: SPR based sensor, optical excitation angle, light coupling technique, Microsystem, Microfluidic

Posted Date: January 20th, 2022

DOI: https://doi.org/10.21203/rs.3.rs-1229043/v1

Design and Optimization of Surface Plasmonic Sensor with Tunable Optical Actuation Angle based on Microsystems Technology for Microfluidic Application

Reza Mokhtarpour, Habib Badri Ghavifekr *

Electrical Engineering Faculty, Sahand University of Technology, Sahand New Town, Iran

*Corresponding author. Tel: 0098-(0)413 345 9375; Fax: 0098-(0)412 344 4322

E-mail addresses: re_mokhtarpour98@sut.ac.ir (Reza Mokhtarpour), badri@sut.ac.ir (Habib Badri Ghavifekr)

*Corresponding author. ORCID: 0000-0003-2834-9821

Abstract

Surface Plasmon resonance-based sensors are one of the most accurate detectors of chemical and biochemical components in microfluidic structures performed based on changes in the refractive index of the medium adjacent to the sensor surface. Precise adjustment of the excitation angle and occupation volume of one kinds of such sensors are among their highlighted challenges that come from conventional light coupling technique. In this paper, a novel idea for designing this type of sensor in microsystem technology is devised, which is capable of adjusting the angle of optical excitation using the thermal-optical effect while it has the minimum occupied volume. This design is optimized and validated using finite element method, so that the sensor performance in exchange for changes in parameters such as Refractive Index, metal Thickness, etc. is examined and displayed in the form of tables and graphs. Simulation results reveal that the proposed model is able to tune optical excitation angle such accurate that the SPR phenomenon occurs at an angle of 21.21˚at the outer boundary of 42 nm thick of gold layer at its best.

Keywords SPR based sensor, optical excitation angle, light coupling technique, Microsystem, Microfluidic

Introduction

In plasmonic sensors, a specific arrangement of optical elements under special conditions, such as the incident angle and the specific wavelength of the input electromagnetic wave, leads to the

coupling of electromagnetic energy to the metal plasmons and the creation of a plasmonic wave on the metal-dielectric interface. The basis of the performance of such sensors is that any change in the refractive index of the medium around the sensor surface leads to a change in the surface plasmonic wave behavior and it reveals informations about the factors of changes in the sensing medium as a result [1-6].

Although optical wave vector is assumed to be at the same direction of SP_s wave vector, surface plasmons cannot be excited by directing the light [5, 6]. It comes from the fact that states the propagation constant of metal surface plasmons is larger than the optical wave propagation constant inherently. In other words. Not only should optical wave vector be parallel to the SP_s wave vector, but also it should be equivalent to the propagation constant of metal surface plasmons. As a result, various models such as prism coupling, waveguide SPR, Diffraction Grating have been proposed to match the propagation constants [6, 7]. In the above models, by using methods such as creation of alternating structure on the metal surface or through embedding another element in the structure, an increase in light wave propagation constant has achieved. In the prism coupling type, by concentrating an electromagnetic wave on a metal-covered dielectric (through embedding a dielectric between the laser and the metal sheet), the incident light wave propagation constant can be increased to match the surface Plasmon propagation constant. The triangular kind of prism and the half-cylindrical lens known as the Kretschmann configuration are such models shown by Fig. 1[1, 2, 5, 6].

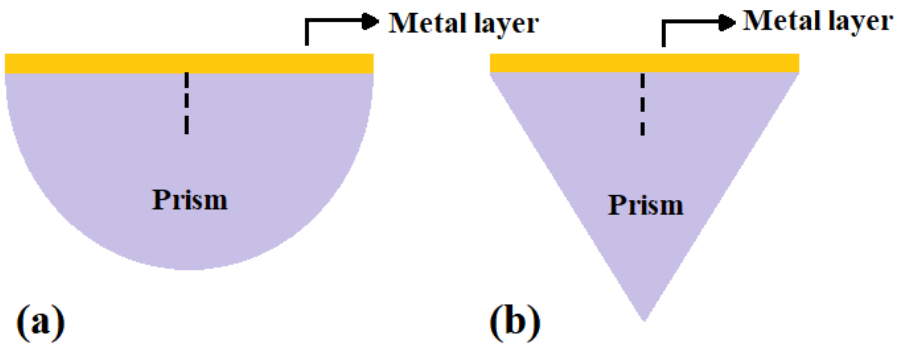

Fig. 1 Conventional models of kretschmann configuration kind of SPR based sensor: (a) the cylindrical lens (b) The triangular prism

In the Kretschmann configuration, the basis of the sensor performance is on the ATR (Attenuated Total Reflection) method. It can be explained by refraction phenomenon in which a light beam passes through a medium with a high refractive index (prism) to an environment with a low refractive index (water). As long as the incident light angle approaches θ_c (critical angle) (Snell's law, $\sin \theta_c = 1$) the light is reflected and refracted to some extent; when the collision angle θ is greater than θ_c, the light is fully reflected and TIR occurs[6]. Meanwhile, if the surface of the glass is covered with a thin layer of metal such as, gold, silver, copper, aluminum, because these metals are conductive and full of energy carriers, and given that the free electrons oscillate at the boundary between the two materials with opposite sign of dielectric coefficients [2], in special conditions (certain angle and wavelength of incoming light) all the light is no longer reflected and part of it disappears in the metal layer, in other words it converts to a plasmonic wave. It should be noticed

that the metal layer thickness should be as short as enough to generated evanescent wave reach to the surface carriers [8].

An angle that is larger than the critical angle at which the reflected light intensity reaches its lowest value and creates a dip in the reflection spectrum is called the excitation angle (θ_{SPR})[1, 6].

By solving the Maxwell equation, oscillation conditions can be expressed as below [5]:

$$k_s = \frac{2\pi}{\lambda} n_p \sin\theta \quad (1)$$

$$k_{sp} = \frac{2\pi}{\lambda}\sqrt{\frac{\varepsilon_m \varepsilon_d}{\varepsilon_m(\varepsilon_m+\varepsilon_d)}} \quad (2)$$

$$k_{sp} = k_s \xrightarrow{yields} \theta_{SPR} = \sin^{-1}\sqrt{\frac{\varepsilon_m \varepsilon_d}{\varepsilon_p(\varepsilon_m+\varepsilon_d)}} \quad (3)$$

Where ε_d, ε_m and η_p represent the complex dielectric constant of the dielectric (sensing medium), the complex dielectric constant of the metal and the refractive index of the dense medium (prism) respectively, and λ is the incident light wavelength.

As it can be seen from Eq. (1), the propagation constant of a surface plasmonic wave at the metal-dielectric interface is heavily dependent on changes in the refractive index of the background medium [5, 6], this feature allows the application of SPR to investigate biochemical reactions occurred near metal surface. This characteristic is explained by a quantity as the sensitivity coefficient of the sensor. Based on the optical property to be measured, the sensitivity of the SPR sensor can be classified into angular modulation, wavelength and intensity modulation [1, 9, 10]. In the most common and sensitive method, known as angular scanning of reflection light, a monochromatic light strikes the metal surface at a wide range of angles, but the surface plasmons at a certain angle absorbs much of the light energy and are triggered and eventually this phenomenon is seen as a dip in the reflection spectrum [1], then any change in the refractive index at the metal-dielectric interface leads to a change in the intensity of the reflection light at the default resonance angle and it causes the displacement of the dip in the reflection light spectrum [6, 9].

$$S = \frac{d\theta_{SPR}}{dn_s} \quad (4)$$

Which is n_s as the refractive index of the sensing medium.

The parameter "Full width at half maximum (FWHM) along with the sensitivity coefficient is another parameter which plays role in determining the quality of the sensor and its accuracy against annoying signals [10].

Detection accuracy represents the fact that how much sensor is able to response to subtle changes of resonance angle come from low concentration of analytes[11].

$$Detection\ Accuracy = \frac{d\theta_{SPR}}{FWHM} \quad (5)$$

$$Quality\ Factor = \frac{Sensitivity}{FWHM} \quad (6)$$

Occurrence of SPP phenomenon is dependent upon the fact whether the coupling of electromagnetic wave is done perfectly or not regarding to coupling technique [12]. It corresponds to what extent SP_s are excited [12]. Thus among the challenges of kretschmann configuration, the limitation in the angular scanning of the incoming light as well as the relatively high occupied volume grab much more attention [7]. Although among the typical models, the cylindrical lens compared to the triangular one supports a larger range of incidence angles of incoming light [12] and also gives a deeper output of the reflection or better output of absorption curve [13], due to the highly dependency of SPR phenomenon formation to the incident light angle, by presenting a model that equipped with innovative coupling technique, it will be shown that better and more precise control over the adjustment of the excitation angle can be achieved. It causes a greater coupling of the electromagnetic waves to the metal, and would eventually results in a better and desirable Reflection and Absorption curve. At the same time, the overall volume of the structure is reduced compared to previous bulky models significantly.

As the Fig. 2 illustrates ,the instruction of this structure is such that when the first diffracted light of grating zone (order1) is transmitted through a Si based substrate with a refractive index of n_{si} = 3.6730 [14], collides with the Th_{Au} =42 nm thick of metal surface at an excitation angle (Θ_{SPR}) and ends in SPW phenomenon. This sensor is installed on a microfluidic channel whose mobile phase is water with refractive index of n_{water}= 1.3180 [14]. Thus, the evanescent plasmonic wave is induced in the microfluidics channel. In this structure, gold is used as a metal layer to improve life expectancy of such sensors because it is more resistive against oxidation than other metals, including silver [6, 13]. Dielectric coefficient of gold layer at the working wavelength is $\varepsilon_d = -115.13 + i * 11.289$ [14, 15].

This design has been evaluated and validated by COMSOL Multiphysics version 5.5 simulation software. In the following sections, the performance of this sensor will be shown by Reflectance and Absorbance diagrams as well as other related parameters as a results of investigating the effects of design parameters such as gold leaf thickness and refractive index changes on its performance.

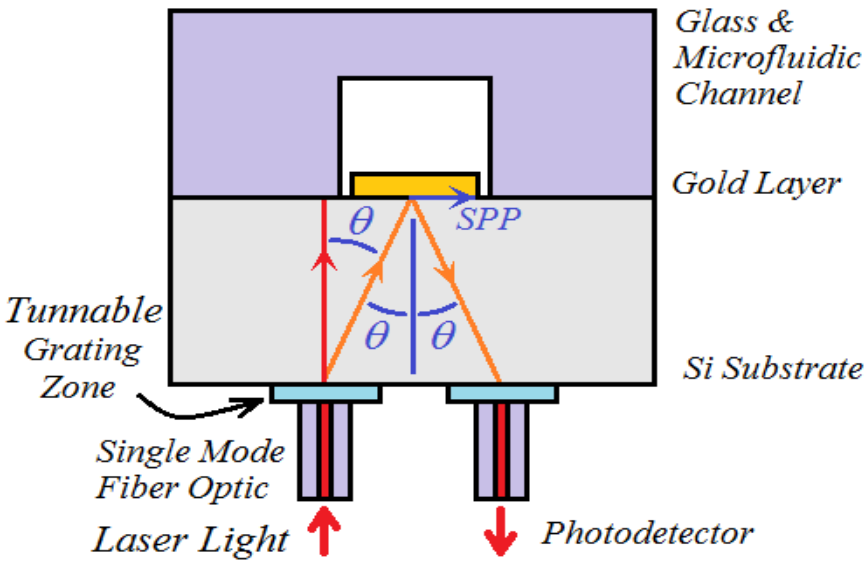

Fig. 2 Schematic of the proposed sensor. Combination of tunable diffraction grating zone which directs light to the metal layer accurately and Si based conventional SPR sensor

An overview of the proposed sensor can be seen in Fig. 2. In accordance with Fig. 2, it combines with light coupling zone and sensing area. The coupling zone is comprised of single mode fiber optic and tunable diffraction grating zone and the sensing part is composed of the main part of conventional SPR sensor (Si based Substrate instead of a prism and the gold layer). This compact is put on the microfluidic channel.

In this structure, Tunable diffraction grating is used to direct the light emitted from single mode fiber optic to the gold layer accurately to results in sharper dip in reflection spectrum. As Fig. 3 shows, desired area constructs of the alternation of polysilicon and epoxy layers in one direction as a grating zone and the thin layer of SiO_2 as an insulator to neutralize the electrical effect of two layers of silicon utilized for grating layer and a substrate.

As it is shown in Fig. 2, when the TM or p-polarized light with a working wavelength of 1550 nm passes through the fiber core with the refractive index $n_{sio2} = 1.444$ [14], strikes the grating surface, So it diffracts into waves with different angles proportion to the grating constant as Eq. (7) represents [16]:

$$m\lambda = d\left(n_\beta \sin\beta - n_\alpha \sin\alpha\right), \qquad -1 \le \sin\theta \le 1 \tag{7}$$

$$\xrightarrow{yields} -(n_\alpha + n_\beta) \le \frac{m\lambda}{d} \le (n_\alpha + n_\beta) \tag{8}$$

Where m is number of orders, d is grating constant or periodicity, n_α and n_β are refractive index of optical fiber core and substrate respectively, α is The angle of incidence of the incoming light to the grating surface and β is The angle of the diffracted waves.

The structure is designed in such a way that when electromagnetic wave hit the grating layer vertically (at $\alpha = 0^\circ$), the first diffracted wave of incident light emits at the excitation angle of the plasmonic sensor (Θ_{SPR}) to create the perfect SPP phenomenon. Thus, Eq. (7) is rewritten as blow as Eq. (9):

$$\alpha = 0 \xrightarrow{yields} m\lambda = d\left(n_\beta \sin\beta\right) \qquad (9)$$

The proposed grating structure is equipped with thermal actuators features for calibration as it is depicted by Fig. 3. It means that due to the very high sensitivity of the plasmonic sensor to the angle of incoming light and according to the Eq. (9) which states that the grating pitch plays role in the diffracted waves angle so through taking fabrication tolerance into account, the angle of first diffracted light (order 1) may not be compatible with the SPP angle. To address this challenge, as shown in Fig. 4, proposed model benefits from the feature as dependency of RI[1] of silicon on temperature [17, 18]. It denotes that the grating zone plays its second role as a thermal actuator to heat in the medium and as a result it induces a gradient in the refractive index of the substrate (n_β) to ultimately have better and more precise control over the adjustment of the diffracted light (order 1) to comply with the Θ_{SPR} . In other word, effect of lack of accuracy in fabrication of grating in its specified pitch size, on diffracted waves angle is compensated by inducing changes in RI.

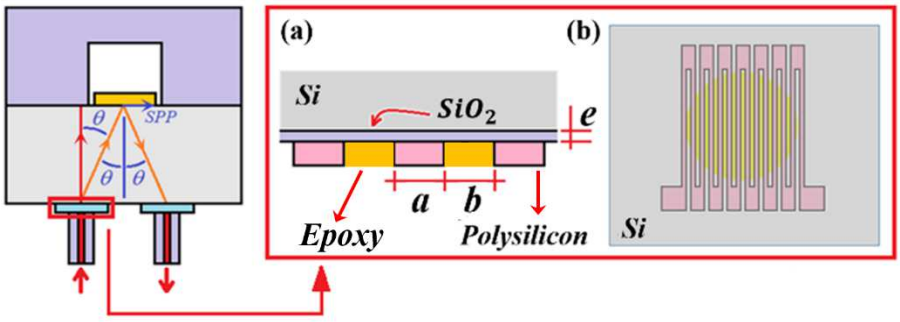

Fig. 3 Tunable diffraction grating zone of proposed sensor: (a) periodicity of polysilicon and epoxy layers above Si based substrate (b) Defining the thermal actuation effects for the diffraction grating zone which can induce changes in refractive index of medium to tune diffracted beams angle more precisely

[1] Refractive Index

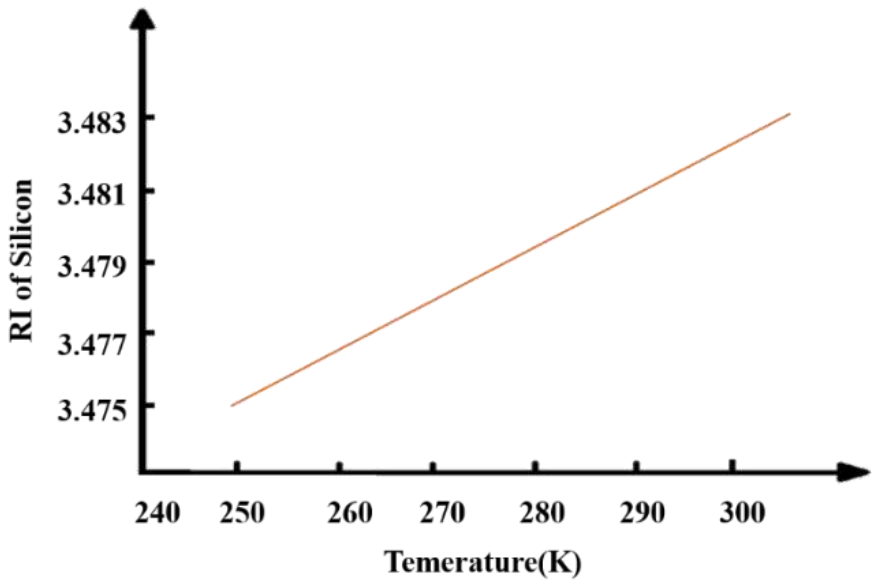

Fig. 4 Temperature dependency of refractive index of silicon at the working wavelength [17]

Results and discussion

In this paper, COMSOL Multiphysics version 5.5 simulation software is used to validate and optimize the performance of this model.

Considering the metal layer as a dissipative material [19], as a first step, the sensor excitation angle is studied through sweeping it across a wide range of incident light angles at the working wavelength of 1550 nm. This is the angle at which the thin sheet of gold absorbs the greatest amount of energy from the incoming light with a phase difference of less than 100°, while the reflectance reaches its lowest value as they can be seen in Fig. 5 and Fig. 6. As Fig. 7 exhibits, surface plasmonic waves generates at a metal-dielectric interface following of this process and it's declined in the sensing medium exponentially.

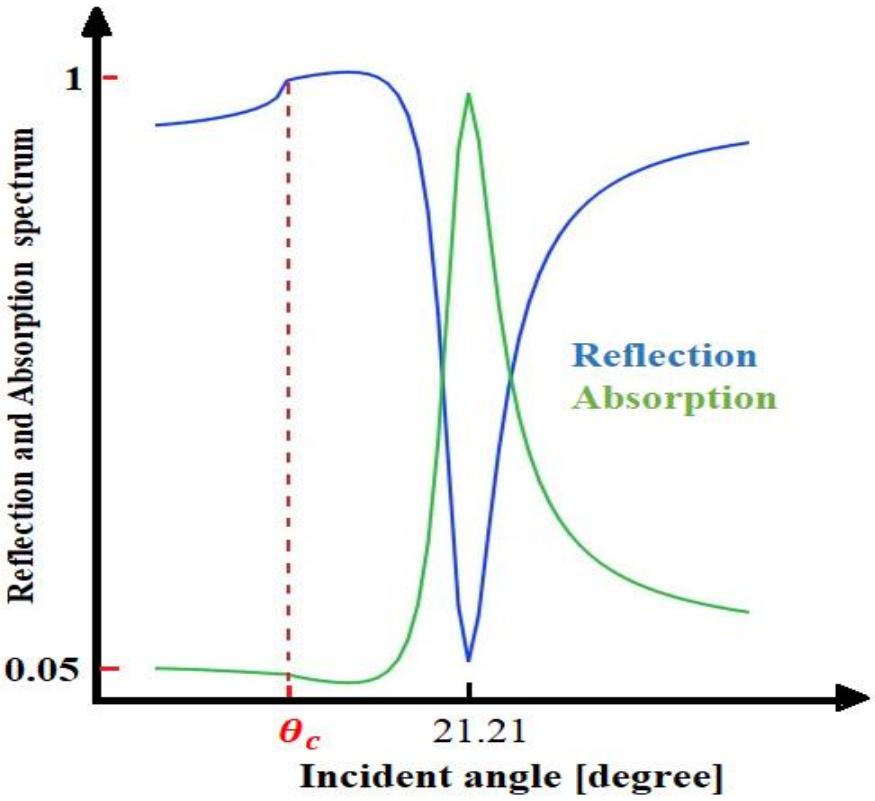

Fig. 5 Reflectance and Absorbance curves in exchange for different angles of incoming light at a constant condition of, λ = 1550 nm and Th_{Au} = 42 nm thick of gold layer

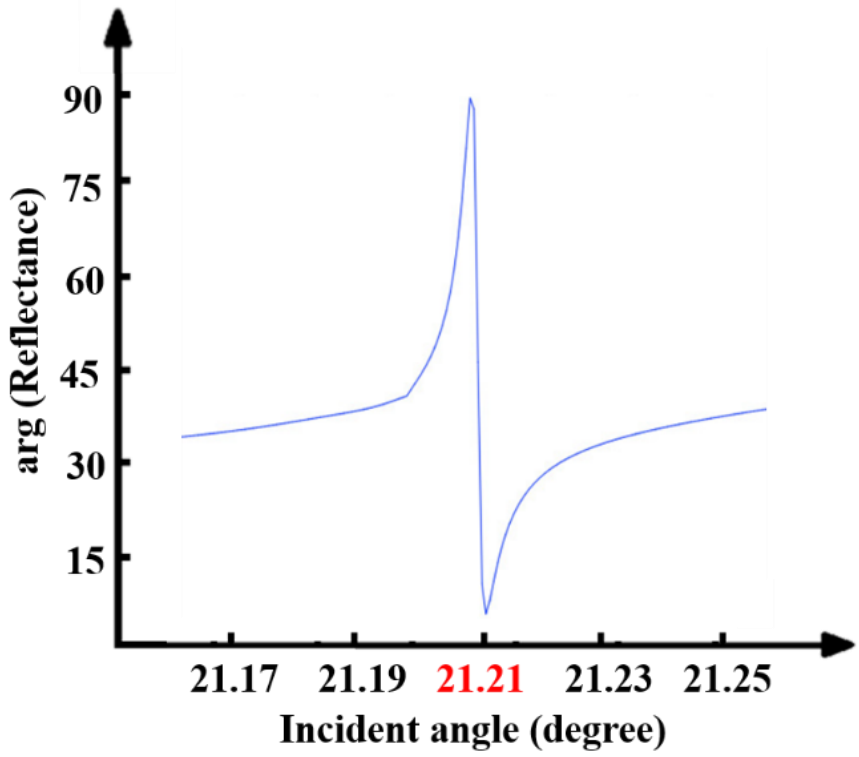

Fig. 6 The phase behavior of the reflected light in exchange for different angles of the incoming light at a constant condition of, λ= 1550 nm and Th_{Au} = 42 nm thick of gold layer. As incoming light angle reaches to the excitation angle, phase of reflected light changes around 100 degree.

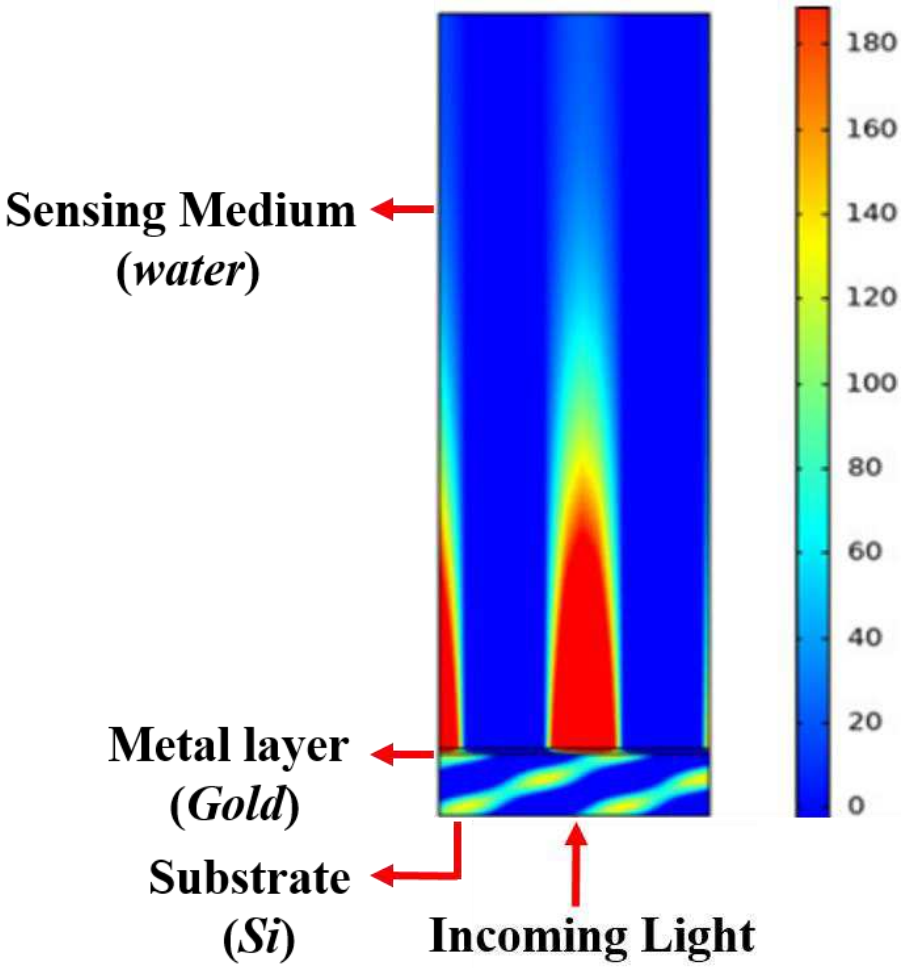

Fig. 7 The portrait of SPW occurrence at the resonance angle of 21.2° on a 42 nm gold surface by striking the light at the wavelength of 1550 nm

When the reflection intensity reaches its minimum value at the resonance angle, an evanescent magnetic field is formed at the metal-dielectric interface, which corresponds to the maximum amount of light absorption by the gold layer. According to the unstable characteristic of generated magnetic field in the vicinity of the metal dielectric interface a penetration depth can be defined for it which discloses the fact how far analytes can be detectable by such sensors. In other words more penetration depth means more interaction volume and results in a higher sensitivity of sensor to the bulk liquid fluctuation.

For this purpose, another simulation was performed to analyses the behavior of the magnetic field at the resonance mode, near the metal-dielectric boundary. Through taking above conditions into

consideration, the sensor sensing range is revealed at its maximum value of 1.498 nm from the metal surface. In other words, this sensor structure is capable of detecting analytes at distances of about 1.498 um from the metal-dielectric interface. It is indicated by

Fig. **8**.

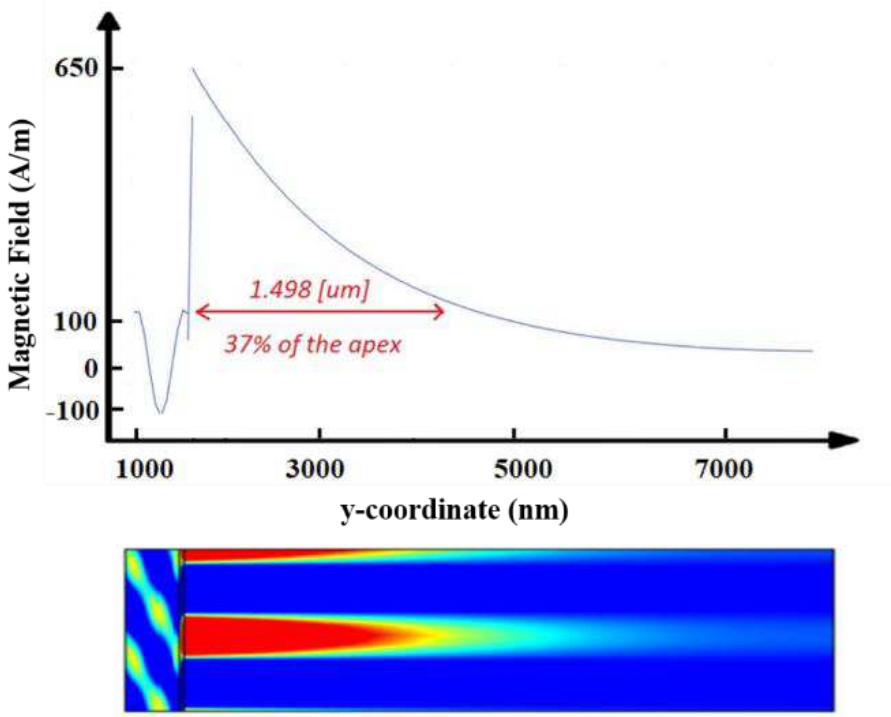

Fig. 8 Distribution of transverse magnetic field (z component) along the sensing medium when light strikes at an angle of 21.2° to a 42 nm thick of gold surface

In optimization of this kind of sensors, another parameter which should be observed is metal thickness [20, 21], because it plays significant role in the quality and detectability of such sensors. Thus the behavior of wave reflected from the gold layer in exchange for different thicknesses of the gold foil following of irradiating of different angles of incoming light is evaluated. It is displayed by Fig. 9.

As Fig. 9 and Fig. 10 indicate the performance of this sensor is at its best in exchange for the 42 nm thick of gold layer. This means that the light emitted at an angle of 21.21° on the gold plate is almost fully coupled to plasmonic waves, and it shows very little reflection, while in this case the FWHM parameter has a smaller size of about 0.08°. This is while FWHM = $\Delta\Theta_{0.5}$ [11] of Reflectance curve increases with decreasing thickness of gold layer revealed by Fig. 9.

It should be noted that the resonance angle of the sensor decreases and shifts to smaller angles with increasing thickness of the gold layer shown by Fig. 11.

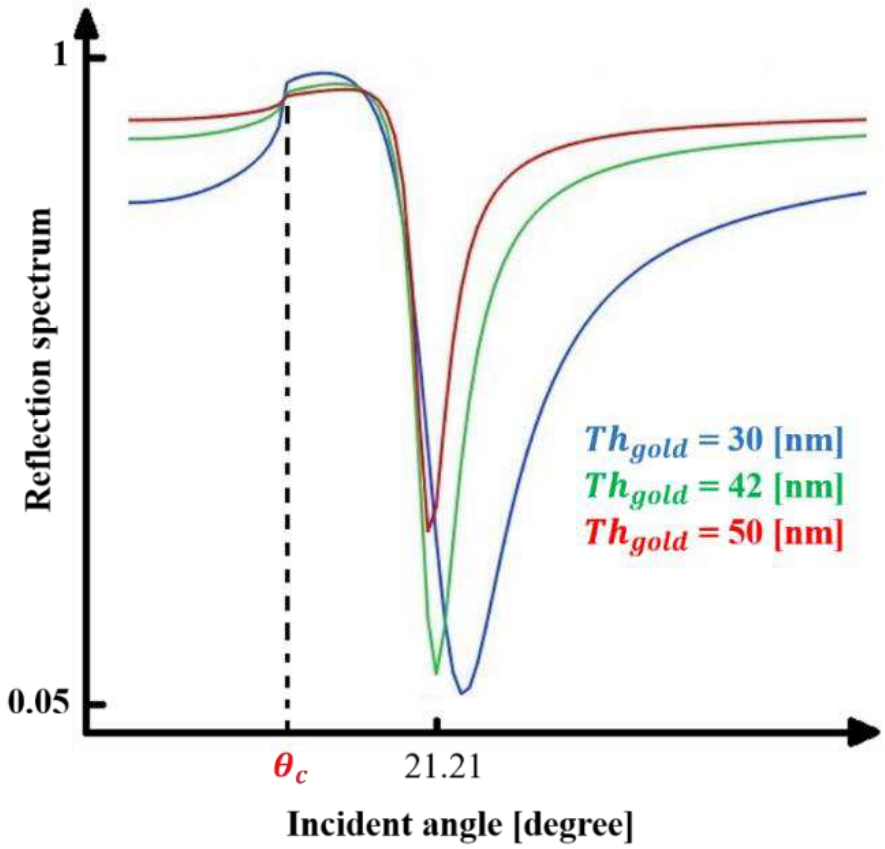

Fig. 9 Reflected light curves from different thicknesses of the gold layer (Th_{gold} = 30, 42, 50 nm) in exchange for irradiating of light at different angles

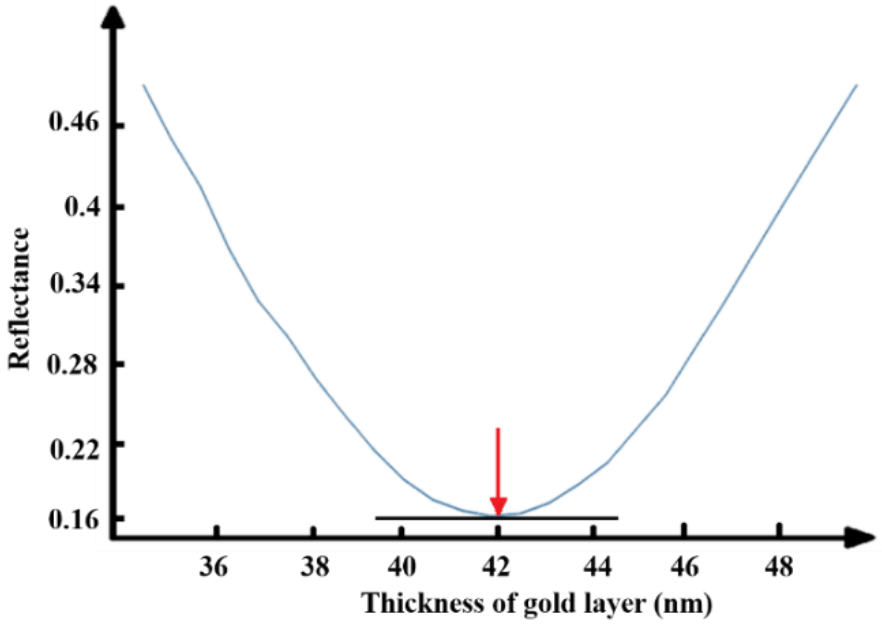

Fig. 10 Changes of Reflection intensity with respect to changes in thickness of gold sheet when light strikes at an angle of 21.2˚

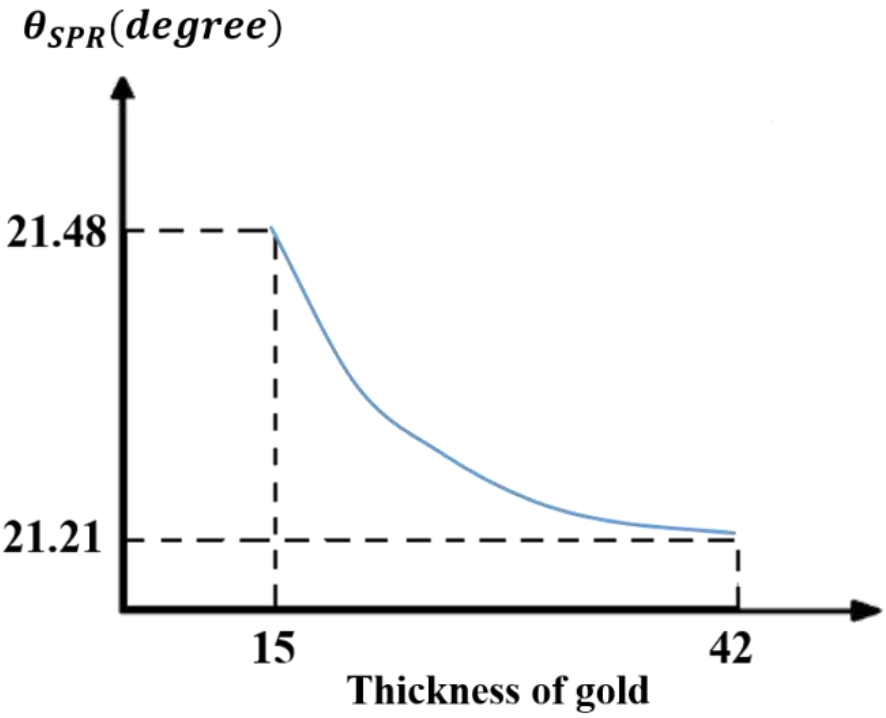

Fig. 11 The curve of resonance angle changes with respect to changes in the thickness of the gold layer

In these conditions, when the analytes pass through the channel and within the sensor sensing region, metal layer free electrons cannot be excited because, as mentioned at the beginning, the performance of this sensor is based on the replying of the SPR phenomenon to the changes in refractive index of sensing medium and as a result contrary to the amplitude of surface plasmonic waves decreased by these changes, these lead to an increase in the amplitude of light reflected from the gold surface, thus making the analytes detectable.

This claim is evaluated through applying changes in RI by $\Delta n = 1\%$ ($n = 1.318 \pm 1\%(1.3180)$) and, as expected, the light reflection intensity at this angle is no longer at its lowest, which indicates a shift in the excitation angle of the sensor; Therefor SPR phenomenon occurs in another angle as can be seen from Fig. 12, Fig. 13 and Table 1.

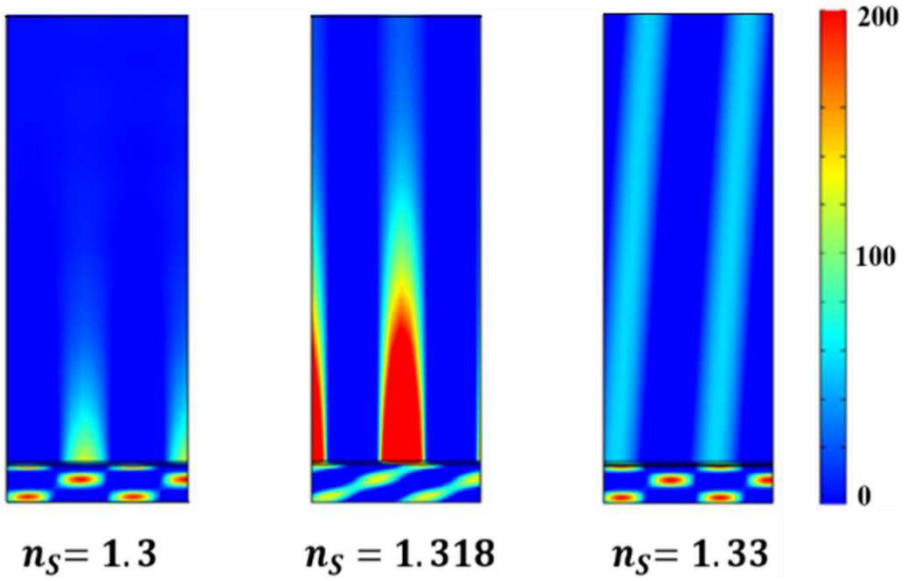

Fig. 12 Diverse responses of Surface Plasmons following by changes in the refractive index of the sensing medium by Δn = 1%, in exchange for incidence of light at the angle of 21.2°

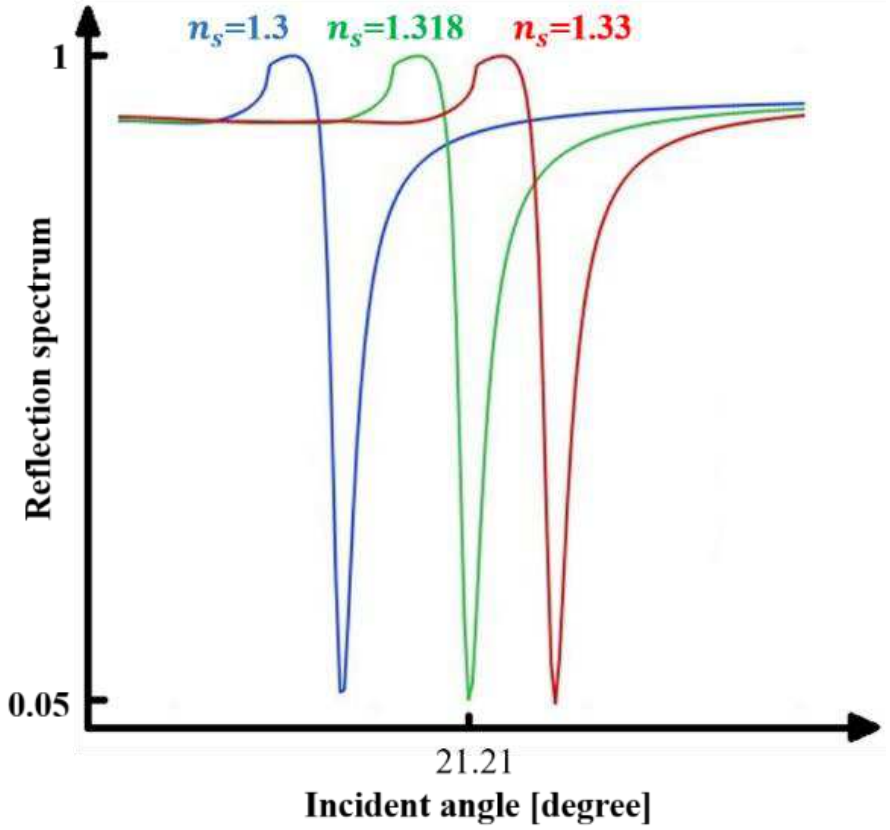

Fig. 13 Different curves of reflection spectrum as a function of incident angle in exchange for changes in the refractive index of the sensing medium by Δn = 1%

Table 1 the amplitude of light reflected from gold surface with thickness of Th_{Au} = 42 nm in exchange for changes in refractive index of sensing medium by Δn = 1%

Refractive Index of sensing medium (n_s)	Reflectance
1.3048	0.82285
1.318	0.05
1.3312	0.89263

Fig. 14 reveals the simulation results as the changes of resonance angle and changes of sensitivity coefficient of sensor at constant condition of Th_{Au} = 42 nm thick of metal layer and λ = 1550 nm, as a function of refractive index of sensing medium. In this figure, as a consequence of changes in refractive index of the sensing medium by 0.02, it can be seen a shift in the angle of formation of surface plasmonic waves by 0.1˚.

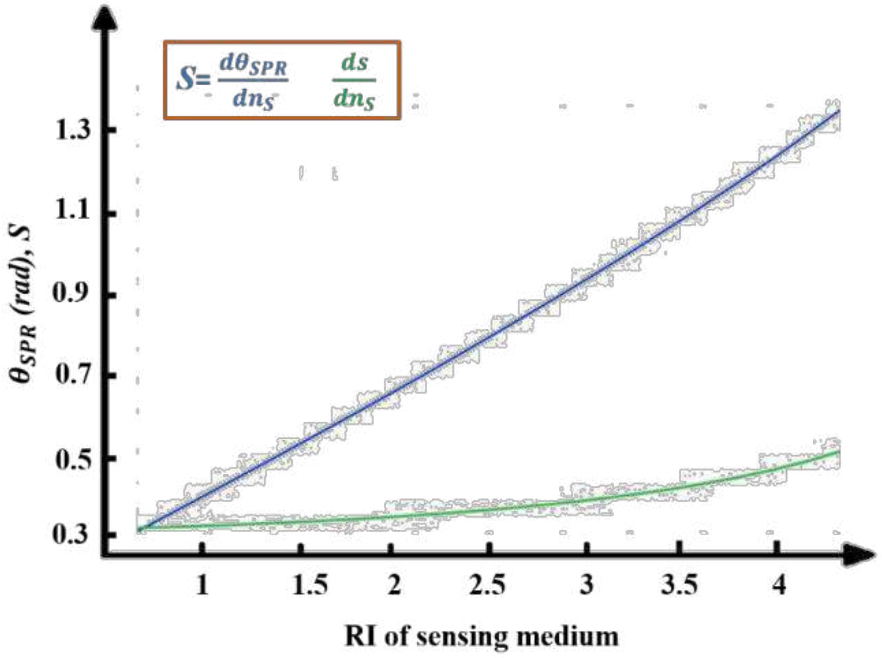

Fig. 14 Curves of resonance angle changes and sensor sensitivity following of changes in the refractive index of the sensing medium

As it is mentioned above, tunable grating zone is put in proposed structure as a novel coupling technique to overcome the conventional challenge of such sensor as failing to irradiate incoming light onto the metal layer at its optimal excitation angle accurately. It works in such a way that when light with a wavelength of λ=1550 nm pass through SiO_2 as a fiber optic core with a refractive index of 1.444, collides with the grating layer with periodic refractive indices n_{epoxy}= 1 and

$n_{polysilicon}$ = 3.6730 vertically. Finally according to Eq. (9) it diffracts into 5 transmission waves at 5 angles in the Si medium as a substrate with a refractive index of n_{si} = 3.6730.

In order for the first diffracted light to be diffracted at the desired angle, the grating constant must be obtained from Eq. (9). Therefore considering the above conditions and given that the surface plasmonic sensor is excited at an angle of Θ_{SPR} =21.2˚, the grating constant is obtained d=1170 nm from Eq. (9). It should be noted that fabrication of such pitch is over production tolerance, so adjustment system is needed to compensate this problem.

This area has also been evaluated and validated in the COMSOL Multiphysics software environment.

The purpose of this work is to investigate the behavior of diffracted transmission waves (T_{-2}, T_{-1}, T_0, T_1, and T_2) in the Si region. As mentioned earlier, this region is designed as to T_1 hit the metal surface at angles around 21.2˚ and result in a spectrum as shown in Fig. 15.

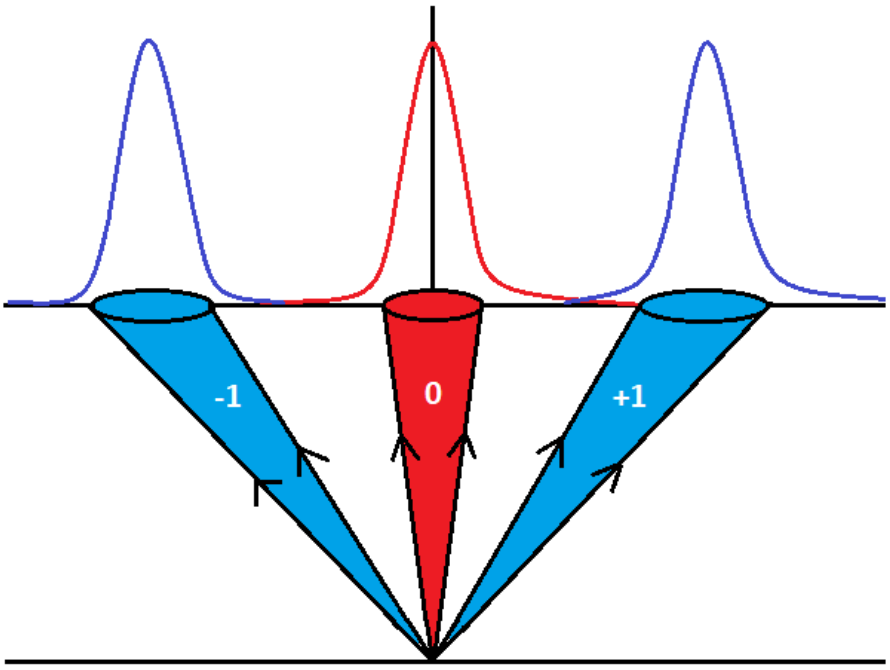

Fig. 15 The spectrum of diffracted transmission waves when the light strikes the grating surface vertically

Initially, as Fig. 16 depicts, 300 nm thick of the grating zone was studied and simulated as a unit cell. Diffracted waves can be sharply focused by increasing the number of grating zone periods. It was Harvey's main part of research done in Aug 2019 [22]. This group has observed a correlation between sharpness and focusing of the diffracted wave and number of periods. To make this achievable it would be better to utilize fiber optic core in size which can cover at least 12 number of periods of actuators. This effect is taken into account by inserting the periodic condition node as a boundary conditions in COMSOL Multiphysics environment, which aims to define such a structure from the side walls infinitely. It gives a much focused result for each of the orders.

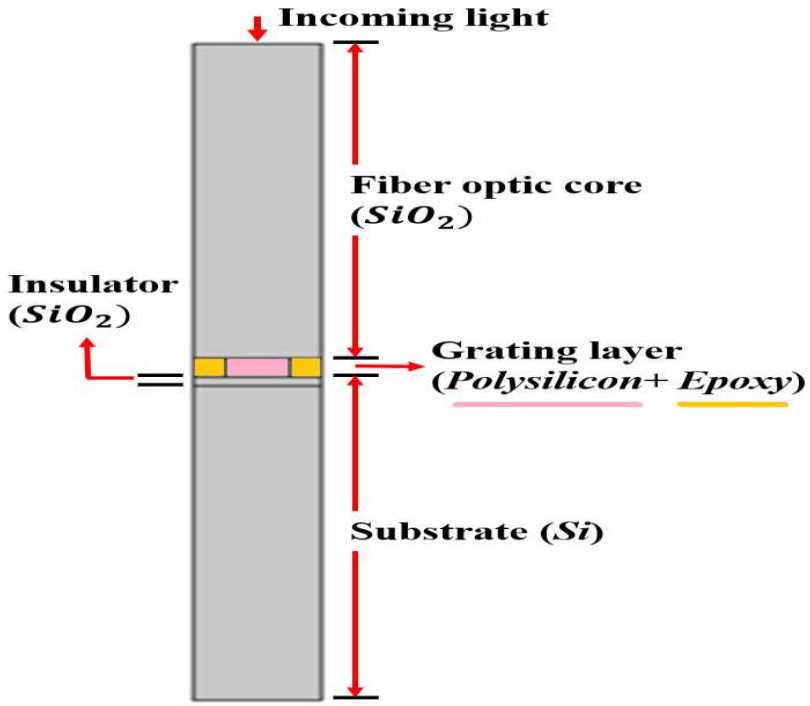

Fig. 16 Schematic of proposed grating zone which is constructed by periodic structure of polysilicon and epoxy layers above the SiO_2 as an insulator to diffract the incoming light into Si based substrate at desired angle

Now that the grating area was designed for a specific excitation angle and an optimal model was obtained, In order to enhance the accuracy of the excitation angle regulation in fabrication process of the sensor, joule heating effects should be defined for that grating zone to induce changes on n_β through heating. As Eq. (9) represents, it results in infinitesimal changes in the angle of the orders and better and more precise control over them. At the first step temperature distribution within the structure was shown by simulating the given thermal actuator role to the optical grating zone in COMSOL Multiphysics environment at Fig. 17 and Fig. 18. This is done by applying electric potential to the thermal-optical effects equipped zone. Fig. 19 and Fig. 20 illustrate, the diffracted waves behavior can be manipulated by changes in RI driven from applying thermal effects.

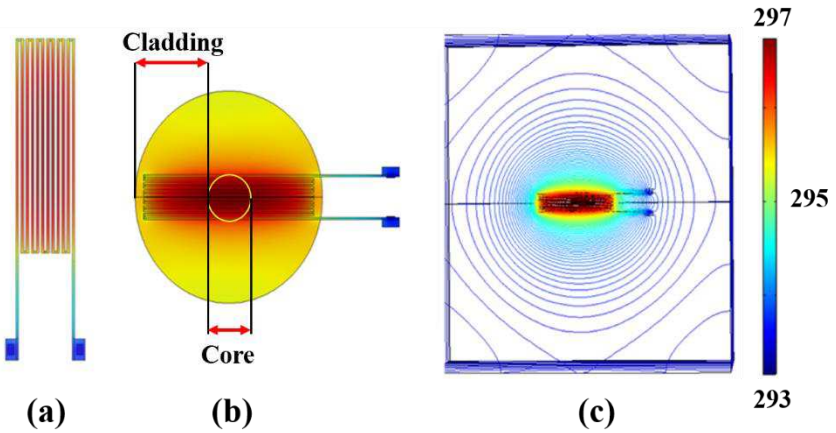

Fig. 17 Temperature distribution across (a) the tunable grating zone (b) the core and cladding of fiber optic (c) the Si-based substrate, as a result of applying the electric potential to the thermo-optic actuators

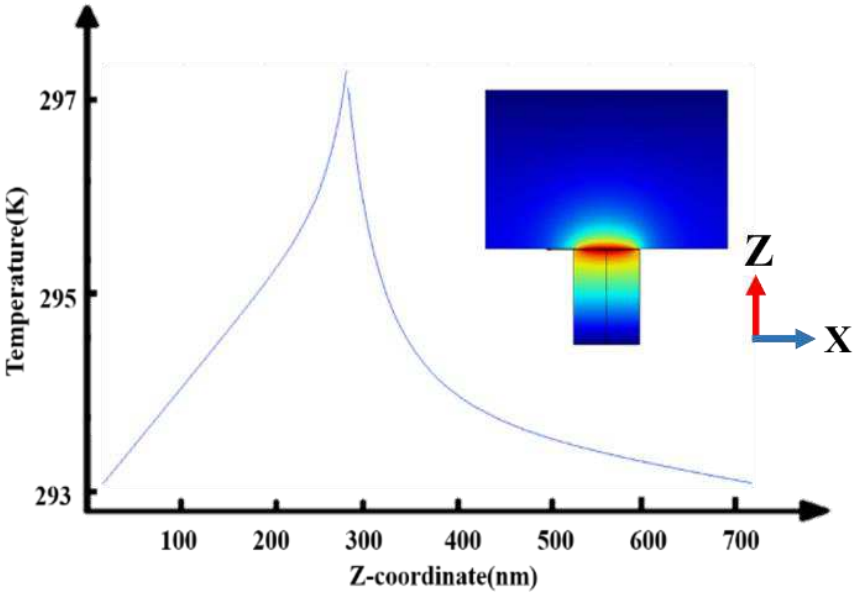

Fig. 18 Curve and schematic of temperature distribution across the proposed sensor

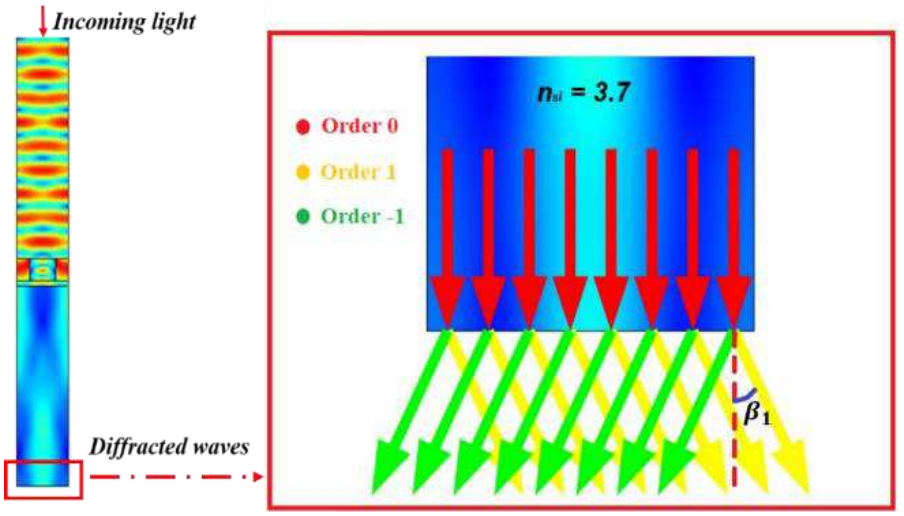

Fig. 19 Schematic of diffracted waves behavior before applying changes in refractive index of substrate (n_s=3.7)

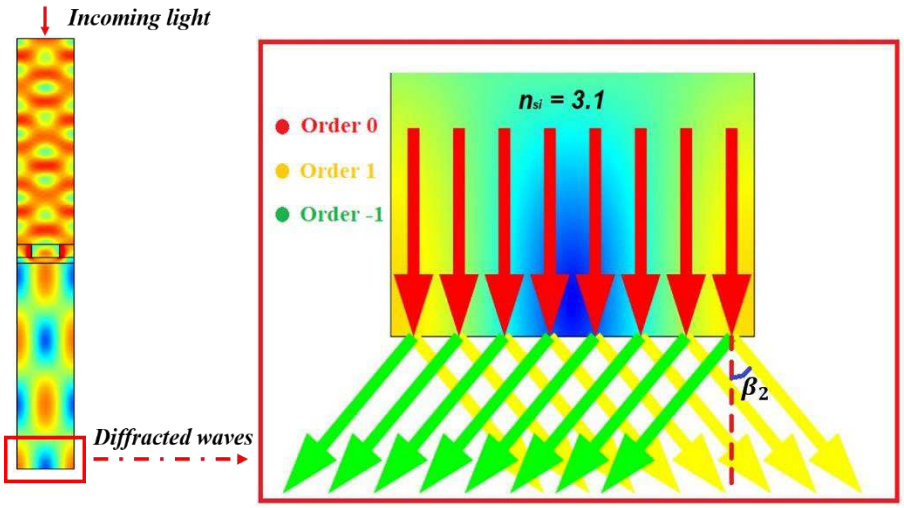

Fig. 20 Schematic of changes in the angles of diffracted waves following induced heat in substrate of sensor (n_s=3.1)

By comparing the Fig. 19 with the Fig. 20, it is revealed that the changes of the n_{si} affects angle of orders desirably. It should be noticed that thermal actuation role of grating zone only causes minor changes in angle of diffracted light waves. Thus, such fluctuations are not able to displace default excitation angle.

Conclusion

Inefficient performance of prism coupling configuration kind of surface plasmonic resonance based sensors relates to the conventional challenge of such sensors in regard to coupling techniques. One of the reasons which regards to this is the lack of precise adjustment of their excitation angle. It means that coupling of electromagnetic wave energy at angles except for Θ_{SPR} cannot be done completely .Therefore light coupling techniques should be modified to address it. In this study, a proposed model demonstrates that by combining a plasmonic sensor with a tunable diffraction grating zone, it can be much easier and accurate to adjust the excitation angle compared to previous models, and results in optimized performance of the SPR sensor. This structure works in such a way, a wave hits the metal surface around the resonance angle of the sensor and causes an energy coupling to its carriers, then defined thermal actuation characteristic of grating zone induces some changes in refractive index of the substrate region. Thus, it intensifies accuracy of incoming light angle which finally lead to fine tuning of the first diffracted transmission wave angle (order 1) to match with Θ_{SPR}. This is how the SPP phenomenon occurs at its best with high quality and resolution. In other word it has illustrated how such design enhances sensor performance and its detection accuracy. In addition, this sensor has a lower occupancy volume compared to conventional models.

Declarations

Funding No funds, grants, or other support was received.

Conflict of Interest The authors declare no conflicts of interest.

Ethics Approval Not applicable.

Consent to Participate Not applicable.

Consent for Publication Both authors consent to publication.

Data Availability and Material Not applicable.

Code Availability Not applicable.

Author Contribution All authors contributed to the study conception and design. Data collection, simulation and analysis of model, results production and writing the manuscript were performed by Reza Mokhtarpour. Both authors made revisions and format manuscript according to the journal guidelines. Habib Badri Ghavifekr is corresponding author and supervised the research project.

References

1. Sharma, S.C., *Surface plasmon resonance sensors: fundamental concepts, selected techniques, materials and applications.* Advances in Sensors; Yurish, S., Ed.; IFSA Publishing: Barcelona, Spain, 2018. **5**: p. 25-77.
2. Homola, J., S.S. Yee, and G. Gauglitz, *Surface plasmon resonance sensors.* Sensors and actuators B: Chemical, 1999. **54**(1-2): p. 3-15.
3. Sambles, J., G. Bradbery, and F. Yang, *Optical excitation of surface plasmons: an introduction.* Contemporary physics, 1991. **32**(3): p. 173-183.
4. Mudgal, N., et al., *Modeling of highly sensitive surface plasmon resonance (SPR) sensor for urine glucose detection.* Optical and Quantum Electronics, 2020. **52**: p. 1-14.
5. Haque, T. and H.K. Rouf. *A performance improved kretschmann configuration based surface plasmon resonance (spr) sensor*. in *2019 1st International Conference on Advances in Science, Engineering and Robotics Technology (ICASERT)*. 2019. IEEE.
6. Miyazaki, C.M., F.M. Shimizu, and M. Ferreira, *Surface plasmon resonance (SPR) for sensors and biosensors*, in *Nanocharacterization techniques*. 2017, Elsevier. p. 183-200.
7. Roh, S., T. Chung, and B. Lee, *Overview of the characteristics of micro-and nano-structured surface plasmon resonance sensors.* Sensors, 2011. **11**(2): p. 1565-1588.
8. Wang, D.-S. and S.-K. Fan, *Microfluidic surface plasmon resonance sensors: From principles to point-of-care applications.* Sensors, 2016. **16**(8): p. 1175.
9. Basak, C., M.K. Hosain, and A.A. Sazzad, *Design and simulation of a high sensitive surface plasmon resonance biosensor for detection of biomolecules.* Sensing and Imaging, 2020. **21**(1): p. 1-19.
10. Homola, J. and M. Piliarik, *Surface plasmon resonance (SPR) sensors*, in *Surface plasmon resonance based sensors*. 2006, Springer. p. 45-67.
11. Singh, Y., M.K. Paswan, and S.K. Raghuwanshi, *Sensitivity Enhancement of SPR Sensor with the Black Phosphorus and Graphene with Bi-layer of Gold for Chemical Sensing.* Plasmonics, 2021: p. 1-10.
12. Mukhtar, W.M., R.M. Halim, and H. Hassan. *Optimization of SPR signals: Monitoring the physical structures and refractive indices of prisms*. in *EPJ Web of Conferences*. 2017. EDP Sciences.
13. Akafzade, H., N. Hozhabri, and S. Sharma, *Highly sensitive plasmonic sensor fabricated with multilayer Ag/Si3N4/Au nanostructure for the detection of glucose in glucose/water solutions.* Sensors and Actuators A: Physical, 2021. **317**: p. 112430.
14. ; Available from: www.refractiveindex.info.
15. Johnson, P.B. and R.-W. Christy, *Optical constants of the noble metals.* Physical review B, 1972. **6**(12): p. 4370.
16. Palmer, C. and E.G. Loewen, *Diffraction grating handbook.* 2005.
17. Frey, B.J., D.B. Leviton, and T.J. Madison. *Temperature-dependent refractive index of silicon and germanium*. in *Optomechanical technologies for Astronomy*. 2006. International Society for Optics and Photonics.
18. Cardona, M., W. Paul, and H. Brooks, *Dielectric constant of germanium and silicon as a function of volume*. 1959: Gordon McKay Laboratory of Applied Science, Harvard University.
19. Alim, N. and M.N. Uddin, *Surface Plasmon Resonance Biosensor in Healthcare Application Using Kretschsmann & Otto Configuration.* AIUB Journal of Science and Engineering (AJSE), 2018. **17**(1): p. 1–6-1–6.
20. Murat, N.F., et al. *Optimization of gold thin films thicknesses in enhancing SPR response*. in *2016 IEEE International Conference on Semiconductor Electronics (ICSE)*. 2016. IEEE.

21. Pluchery, O., R. Vayron, and K.-M. Van, *Laboratory experiments for exploring the surface plasmon resonance.* European journal of physics, 2011. **32**(2): p. 585.
22. Harvey, J.E. and R.N. Pfisterer, *Understanding diffraction grating behavior: including conical diffraction and Rayleigh anomalies from transmission gratings.* Optical Engineering, 2019. **58**(8): p. 087105.